12-1-2003

Sorption in Proton-Exchange Membranes - An Explanation of Schroeder's Paradox

P. H. Choi

Ravindra Datta
Worcester Polytechnic Institute, rdatta@wpi.edu

Journal of The Electrochemical Society, **150** (12) E601-E607 (2003)
0013-4651/2003/150(12)/E601/7/$7.00 © The Electrochemical Society, Inc.

Sorption in Proton-Exchange Membranes

An Explanation of Schroeder's Paradox

Pyoungho Choi and Ravindra Datta*,z

Fuel Cell Center, Department of Chemical Engineering, Worcester Polytechnic Institute, Worcester, Massachusetts 01609, USA

A physicochemical model is proposed to describe sorption in proton-exchange membranes (PEMs), which can predict the complete isotherm as well as provide a plausible explanation for the long-unresolved phenomenon termed Schroeder's paradox, namely, the difference between the amounts sorbed from a liquid solvent *vs.* from its saturated vapor. The solvent uptake is governed by the swelling pressure caused within the membrane as a result of stretching of the polymer chains upon solvent uptake, Π_M, as well as a surface pressure, Π_σ, due to the curved vapor-liquid interface of pore liquid. Further, the solvent molecules in the membrane are divided into those that are chemically, or strongly, bound to the acid sites, λ_i^C, and others that are free to physically equilibrate between the fluid and the membrane phases, λ_i^F. The model predicts the isotherm over the whole range of humidities satisfactorily and also provides a rational explanation for the Schroeder's paradox.
 [DOI: 10.1149/1.1623495]

Manuscript submitted February 18, 2003; revised manuscript received May 23, 2003. Available electronically October 23, 2003.

Fuel cells based on proton-exchange membranes (PEMs) are of great potential as efficient and largely pollution-free power generators for mobile and stationary applications.[1-3] The PEM fuel cell comprises a membrane electrode assembly (MEA) involving two carbon cloth (or paper) gas-diffusion layers that allow simultaneous transport of gases and water while collecting current, and two carbon-supported Pt or Pt alloy catalyst layers where the electrochemical reactions take place, sandwiching a PEM that allows protons to transfer from the anode to the cathode. The membranes, typically a perfluorosulfonic acid (PFSA) polymer such as Nafion, consist of a polytetrafluoroethylene (PTFE) backbone with side chains terminating in $SO_3^-H^+$ groups. They possess little porosity in the dry state. However, in the presence of water or other polar solvents, the membrane swells and the sulfonic acid groups ionize, protonating the sorbed solvent molecules responsible for conducting the protons.[4,5] The conductivity of Nafion is highly dependent upon hydration level,[6,7] being essentially an insulator below a threshold and rising through several orders of magnitude to about 0.07-0.1 S/cm at 80°C when fully hydrated.[4-7] The extent of the solvent uptake and membrane swelling is controlled by a balance between the internal osmotic pressure of solvent within the pores and the elastic forces of the polymer matrix which, in turn, depend upon the temperature and membrane pretreatment.[8] The membrane pretreatment involves raising the temperature to around the glass transition temperature of Nafion (111°C) to allow the polymer chains to reorient themselves in the presence of water.[9] The membrane is first cleaned in a boiling 3% H_2O_2 solution, followed by boiling in 0.5 M H_2SO_4 to ensure full protonation, and finally in deionized water. This results in the so-called E (expanded) form. Other pretreatment procedures that have been described in the literature include drying at 80°C that produces the N (normal) form, while drying at 105°C produces the S (shrunk) form.[10]

The results of water uptake in Nafion expressed in terms of λ, the number of water molecules per acid site, upon contact with liquid or its saturated vapor are summarized in Table I. There is an unexplained discrepancy in the water uptake in Nafion from pure liquid ($\lambda_{i,L}^{sat} \approx 22$-23) *vs.* that from its saturated vapor ($\lambda_{i,V}^{sat} \approx 13.5$-14.0), even though both possess unit activity.[11-18] In fact, when a liquid water-equilibrated membrane was removed and exposed to a saturated water vapor, λ dropped from 22 to 14, indicating that the two states are thermodynamically stable.[11] The phenomenon, known as Schroeder's paradox,[19] is apparently not uncommon in polymer systems but has not so far been satisfactorily explained, although many different explanations have been advanced.[20-29] For instance, it has been attributed to the failure of achieving the same temperature in the saturated vapor as in the liquid phase,[20-22] the low permeation rate of vapor phase adsorption,[23,24] the existence of a metastable state that is sensitive to slight changes in experimental conditions,[25] structure and rigidity effects of solid substances,[26] insufficient time of vapor adsorption,[21,26] and poor wetting of the condensates on solid substances.[11] However, these disparate explanations do not provide a satisfactory and general understanding of the phenomenon.

It is important to understand the solvent uptake by PEMs so that fuel cell design and operation can be optimized, which is the objective of this paper. The sorption of water in Nafion has been modeled based on a finite-layer Brunauer-Emmett-Teller method (BET),[5] modified BET,[30] Flory-Huggins,[30,31] or simply fitted using polynomials in activity.[18,32] A sorption model of water in Nafion is proposed here based on the premise that the sorption isotherm is controlled by the swelling pressure determined by the matrix and surface forces of the polymer membrane and sorbed solvent, which in turn affects its chemical potential, and hence the amount sorbed.

Model Description

When an ion-exchange membrane, *e.g.*, Nafion, is in equilibrium with a solvent, *e.g.*, water, some of the sorbed solvent molecules are in a physicochemical state that is different from the bulk solvent molecules depending upon their interaction with the membrane. Thus, the sorbed molecules may be associated with: (*i*) the ion-exchange site, *e.g.*, sulfonic acid group; or (*ii*) the polymer matrix, *e.g.*, fluorocarbon backbone in Nafion; or (*iii*) the other solvent molecules. In the model developed here, we simply assume that the sorbed solvent molecules are of two types: (*i*) those that are strongly, or chemically, bound to the acid sites in the primary solvation layer, akin to chemisorption; and (*ii*) others that are physically equilibrated between the fluid and the membrane phases, akin to physisorption. In other words, we do not explicitly account for the solvent interactions with the polymer backbone in this treatise, which is included in the effective spring constant κ of the polymer matrix. It is further assumed that as the membrane swells due to solvent uptake, the solvent molecules meet increasing resistance from the stretched polymer chains, resulting in a swelling pressure on the pore liquid. The pressure alters the solvent chemical potential within the membrane, and hence the sorption equilibrium. When the sorption occurs from the vapor phase, an additional pressure is exerted on the pore liquid by the curved vapor-liquid interface within the pore. This latter effect is invoked here to explain Schroeder's paradox.

* Electrochemical Society Active Member.
z E-mail: rdatta@wpi.edu

Table I. The amount of water sorption in Nafion by liquid water and its saturated vapor at about room temperature.[a]

Number of water molecules per sulfonic acid, λ_i^{sat}	
Liquid	Vapor
22 (25°C)[11,12]	13.5 (25°C)[14]
22.6 (25°C)[13]	13.5 (25°C)[18]
23 (25°C)[15]	13.6 (25°C)[16]
22.3 (25°C)[17,b]	14 (30°C)[11,12]

[a] The data reported are for proton-exchanged *E* form of Nafion membrane. All data are for Nafion 117 except b.
[b] Nafion 120 (ion-exchange capacity is 0.83 mequiv/g dry proton-exchanged form and thickness is 250 μm). Temperatures of the experiments are given in parenthesis and references are in superscript.

The model thus involves a balance of forces.[33,34] Equilibrium is achieved when the elastic pressure of the polymer matrix counterbalances the increased pressure within the pore liquid in an effort of solvent molecules to equalize the chemical potential of the fluid inside and outside the pore. Figure 1 shows a schematic of the polymer matrix in its dry (unswollen) and stretched (swollen) states. The effective spring constant κ of the polymer matrix, much like its Young's modulus, is assumed to depend upon the temperature (*e.g.*, proximity to the glass-transition temperature, T_g), solvent-polymer interaction, and pretreatment procedures. Above the T_g the membrane would lose integrity, eventually forming a dispersion of the polymer in the solvent, *e.g.*, Nafion gel.[4] Thus, it can be envisioned that the other key variables that affect swelling are (*i*) the polarity of the solvent, (*ii*) the nature, *e.g.*, hydrophobicity, of the polymer backbone, (*iii*) the concentration of the acid sites, and (*iv*) the strength of the acid sites.[35]

Theoretical Model

The sorbed molecules are assumed to be of two types: (*i*) those that are chemically, or strongly, bound (akin to chemisorption), represented by λ_i^C; and (*ii*) those that are "free" to physically equilibrate (akin to physisorption) between the membrane and the fluid phase, λ_i^F. A schematic of these two different types of water molecules in Nafion is shown in Fig. 2. Thus, the total uptake of solvent by the membrane (number of solvent molecules sorbed/ion exchange site) is written as

$$\lambda_i = \lambda_i^C + \lambda_i^F \quad [1]$$

The thermodynamic condition for the "chemical" equilibrium that determines λ_i^C is

$$\sum_{i=1}^{n} \nu_{\rho i}\mu_i = 0 \quad (\rho = 1, 2, \ldots, q) \quad [2]$$

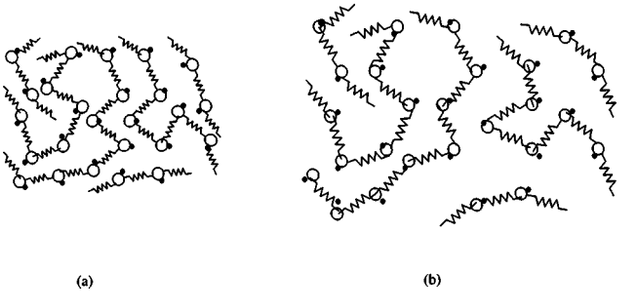

Figure 1. Schematic representation of an ion-exchange membrane in its (a) unswollen and (b) swollen state. The (○) fixed and (●) counterions in the membrane.

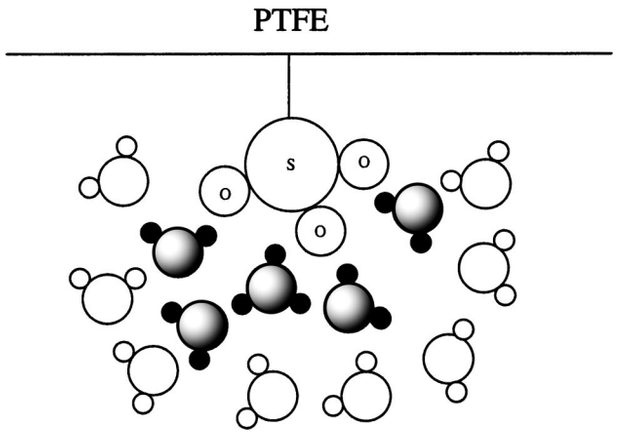

Figure 2. The two types of sorbed water molecules in the PEM: five strongly bound water molecules in the primary hydration shell, akin to chemisorption, and eight free water molecules, akin to physisorption.

where $\nu_{\rho i}$ and μ_i designate the stoichiometric number of species i in reaction ρ and the chemical potential of species i in solution, respectively. The thermodynamic conditions for describing phase equilibrium between the membrane and external fluid phases are

$$\mu_{i,M} = \mu_{i,F} \quad (i = 1, 2, \ldots, n) \quad [3]$$

which determines λ_i^F.

The general chemical potential for species i ($i = 1, 2, \ldots, n$) in phase α can be written as a function of temperature, pressure, composition, and other potentials, $\mu_{i,\alpha} = (T, P, a_{i,\alpha}, \Psi_{i,\alpha})$, *e.g.*

$$\mu_{i,\alpha} = \mu_i^\circ(T, P^\circ) + \int_{P^\circ}^{P} (\overline{V}_{i,\alpha})dP + RT \ln a_{i,\alpha} + \Psi_{i,\alpha} \quad [4]$$

where $\mu_i^\circ(T, P^\circ)$ is the standard chemical potential of species i (*e.g.*, for unit activity), T is the temperature, P° is the standard pressure, $\overline{V}_{i,\alpha}$ is the partial molar volume of i, $a_{i,\alpha}$ is the activity of i, and $\Psi_{i,\alpha}$ represents other potentials in the phase α. For example, when an electrostatic potential ϕ exists in a given phase, for a charged species i

$$\Psi_i = z_i F\phi \quad [5]$$

where z_i is the charge number of species i and F is Faraday's constant.[35,36] The solvents of interest here do not contain any ionic species.

Liquid-membrane phase equilibria.—For equilibration between a liquid and membrane phase for an uncharged species i, the use of Eq. 3 and 4 for an incompressible solvent leads to

$$\ln \frac{a_{i,M}^F}{a_{i,L}} = -\left(\frac{\overline{V}_i}{RT}\right)\Pi_M \quad [6]$$

where the membrane swelling, or osmotic pressure, $\Pi_M = P_M - P_L$, is the pressure rise within the membrane exerted by the polymer matrix due to stretching to accommodate the imbibed pore liquid.[35,37] Many theoretical models have been proposed for the osmotic pressure,[38-40] which is known to vary as a function of the ionic concentration of solution and elastic network of solid substance.[41] The activity of species i within the membrane $a_{i,M}^F$ corresponds to the free, or nonchemically bound, molecules of i, as denoted by the superscript *F*.

Vapor-membrane phase equilibria.—When the membrane equilibrates with a vapor phase, assuming that the pressure changes within

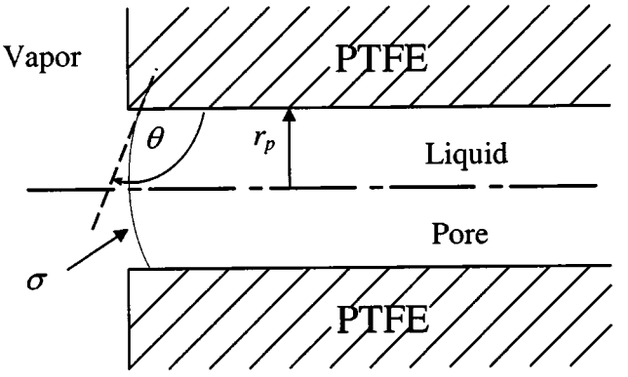

Figure 3. Schematic representation of absorbed solvent in the pore when membrane contacts with vapor-phase environment.

the condensed phase in the pore are caused both by the stretching of the polymer network upon solvent uptake, Π_M, as well as that exerted by the curved vapor-liquid interface within the pores, Π_σ, use of Eq. 3 and 4 results in

$$\ln \frac{a^F_{i,M}}{a_{i,V}} = -\left(\frac{\overline{V}_i}{RT}\right)(\Pi_M + \Pi_\sigma) \quad [7]$$

where the vapor phase activity $a_{i,V} = P_i/P_i^{sat}$, where P_i is the partial pressure and P_i^{sat} is the vapor pressure of solvent. Π_σ is provided by the equation of Young and Laplace[42,43]

$$\Pi_\sigma = -\frac{2\sigma \cos\theta}{r_p} \quad [8]$$

where θ is the liquid-membrane contact angle and r_p is the mean pore radius of liquid-filled pores as shown in Fig. 3. For the case of saturated vapor, $P_i = P_i^{sat}$, Eq. 8 gives

$$\ln\ a^F_{i,M} = -\left(\frac{\overline{V}_i}{RT}\right)(\Pi_M + \Pi_\sigma) \quad [9]$$

whereas for the case of pure liquid solvent i, from Eq. 6

$$\ln\ a^F_{i,M} = -\left(\frac{\overline{V}_i}{RT}\right)\Pi_M \quad [10]$$

It is then clear from Eq. 9 and 10 that, in general, the amount sorbed from a saturated vapor would be different from that sorbed from a pure liquid, both possessing unit activity. This simple result provides a plausible explanation for Schroeder's paradox for the sorption in polymers.

Simplifying assumptions.—The previous equations are largely free of assumptions. However, in order to use these results for predictive purposes, it is assumed here that the activity coefficients of the physically equilibrated species within the membrane are the same as those in the liquid phase.[40] Then, for the liquid phase sorption in Eq. 6, $a^F_{i,M}/a_{i,L} = \gamma^F_{i,M}x^F_{i,M}/\gamma_{i,L}x_{i,L} \approx x^F_{i,M}/x_{i,L}$

$$\ln \frac{x^F_{i,M}}{x_{i,L}} = -\left(\frac{\overline{V}_i}{RT}\right)\Pi_M \quad [11]$$

The mole fraction of the free solvent molecules within the membrane is[35,44,45]

$$x^F_{i,M} = \frac{\lambda^F_i}{\lambda^F_i + 1} \quad [12]$$

It is next assumed that swelling pressure exerted within the pores is linear in solvent uptake[33-35,46]

$$\Pi_M = \kappa\varepsilon \quad [13]$$

where the effective spring constant κ is a function of the elasticity of the polymer network, degree of cross-linking, interaction between polymer network and solvent, temperature, and membrane pretreatment and history. The pore volume fraction occupied by the liquid, ε, is[5]

$$\varepsilon \approx \frac{\lambda_i}{\frac{V_M}{V_i} + \lambda_i} \quad [14]$$

where $\overline{V}_M$ and $\overline{V}_i$ are partial molar volumes of membrane and solvent, respectively. Finally, it is assumed that the pore radius of liquid-filled pores may be estimated using the parallel pore model

$$r_p \approx \frac{2\varepsilon}{S} \quad [15]$$

The pore specific surface S (m^2/cm^3 membrane) is assumed not to vary substantially with increasing uptake. These assumptions when utilized in the previous expressions provide a predictive model for the phase equilibrium between membrane and liquid (or vapor) phase in terms of common physical properties along with the empirical spring constant, κ.

It has been further reported that the contact angle of water in Nafion 117 membrane varies systematically with the hydration level.[47] Thus, for a completely dry membrane, $\theta = 116°$, which is close to that for PTFE, indicating substantial hydrophobicity. The contact angle decreases gradually at first with θ, and then somewhat more sharply, reaching $\theta = 98°$ for vapor saturated membrane with $\lambda^{sat}_{i,V} = 14$, indicating gradually increasing hydrophilicity.

Chemical equilibria.—Equation 2 and 4 when combined yield the usual chemical equilibrium for reaction ρ

$$K_\rho = \exp\left(\frac{-\Delta G^\circ_\rho}{RT}\right) = \prod_{i=1}^{n} a_i^{\nu_{\rho i}} \quad [16]$$

where K_ρ is the equilibrium constant for reaction ρ and $\Delta G^\circ_\rho \equiv \Sigma_{i=1}^{n}\nu_{\rho i}G^\circ_i(T, P)$ is the standard Gibbs energy change. Formation of the hydration shell may be described by stepwise equilibrium, and the binding of solvent molecules in the shell is assumed to occur by the sequential reactions between the polymer acid groups A^-H^+ and polar solvent molecules BOH (*e.g.*, HOH, CH_3OH) as evidenced by IR spectroscopic analysis[48]

$$A^-H^+ + BOH \rightleftharpoons A^-BOH_2^+ \quad K_1 \quad [17]$$

$$A^-BOH_2^+ + BOH \rightleftharpoons A^-BOH_2^+(BOH) \quad K_2 \quad [18]$$

$$A^-BOH_2^+(BOH) + BOH \rightleftharpoons A^-BOH_2^+(BOH)_2 \quad K_3 \quad [19]$$

$$A^-BOH_2^+(BOH)_{\nu-2} + BOH \rightleftharpoons A^-BOH_2^+(BOH)_{\nu-1} \quad K_\nu \quad [20]$$

where ν corresponds to the total number of equilibrium steps for the successive equilibrium reaction for the primary solvation shell. The first of these, for instance, represents dissociation of the polymer-bound acid group and concomitant protonation of the solvent forming, *e.g.*, hydronium ion, whereas the second and subsequent steps represent further solvation. In order to distinguish between chemical and physical equilibrium, the solvent molecules with $K_j \geqslant 1$ are considered to be strongly bound,[49] and the interactions of an acid site with solvent molecules for $K_j \leqslant 1$ are assumed weak enough to

be accounted for by physical equilibration. Using Eq. 16 for these and replacing activities of chemisorbed sites by their fraction of total number of acid sites

$$\theta_1 = K_1\theta_0 a_i; \quad \theta_2 = K_2\theta_1 a_i = K_1K_2\theta_0 a_i^2;$$
$$\theta_3 = K_1K_2K_3\theta_0 a_i^3 \ldots \text{etc.} \qquad [21]$$

such that the *j*th term

$$\theta_j = K_j\theta_{j-1}a_i = \left(\prod_{\rho=1}^{j} K_\rho\right)\theta_0 a_i^j \qquad [22]$$

where θ_j refers to the fraction of acid sites with j strongly bound solvent molecules. Combining this with total ion-exchange site balance, the isotherm for the strongly bound solvent molecules

$$\lambda_i^C = \frac{\Sigma_{j=1}^{\nu}(\Pi_{\rho=1}^{\nu}K_\rho)j(a_i)^j}{1 + \Sigma_{j=1}^{\%\nu}(\Pi_{\rho=1}^{\nu}K_\rho)(a_i)^j} \qquad [23]$$

The use of this expression requires the knowledge of ν equilibrium constants. In order to reduce the number of parameters required for predictions, two simpler cases are considered:

1. If it is assumed that all $K_\rho = K_1$, *i.e.*, all molecules sorb equally strongly, then Eq. 23 simplifies to

$$\lambda_i^C = \frac{K_1 a_i}{1 - K_1 a_i}\left(\frac{1 - (\nu + 1)(K_1 a_i)^\nu + \upsilon(K_1 a_i)^{\nu+1}}{1 - (K_1 a_i)^{\nu+1}}\right) \qquad [24]$$

2. Clearly, $K_1 \gg K_2 \gg K_{j-1} \gg K_j$, as the energy of interaction decreases quickly with the number of the strongly bound molecules/site. Thus, the proton affinity of each subsequent water molecule drops rapidly. Therefore, if it is assumed that ΔG_ρ° in Eq. 16 is proportional to the inverse ρ^q, *e.g.*, $q = 3$ corresponding to dispersion interactions,[43] then

$$\prod_{\rho=1}^{\nu} K_\rho = \exp\left[-\frac{\Delta G_1^\circ}{RT}\left(\sum_{\rho=1}^{j}\frac{1}{\rho^q}\right)\right] \approx K_1 \qquad [25]$$

because the sum of the series is not substantially greater than unity (*e.g.*, for $q = 3$ and $j = 5$, it is 1.1856). Using this approximation in Eq. 23, *i.e.*, all $K_\rho = 1$ except K_1, the simplified isotherm for the strongly sorbed molecules is

$$\lambda_i^C = \frac{K_1 a_i}{1 - a_i}\left(\frac{1 - (\nu + 1)(a_i)^\nu + \upsilon(a_i)^{\nu+1}}{1 + (K_1 - 1)a_i - K_1(a_i)^{\nu+1}}\right) \qquad [26]$$

In reality, the individual equilibrium constants for the successive absorption of solvent molecules drop less quickly. For instance, the first and second ones, and sometimes even third and fourth depending on the type of ions, are significant compared with the rest of the equilibrium constants.[49,50]

Both Eq. 24 and 26 have the virtue of involving only two parameters, namely, K_1 and ν. Since the reality would lie somewhere between the two extremes represented by these expressions, the intermediate case is represented by a slight modification of Eq. 26, *i.e.*,

$$\lambda_i^C = \lambda_{i,m}\frac{K_1 a_i}{1 - a_i}\left(\frac{1 - (\nu + 1)(a_i)^\nu + \nu(a_i)^{\nu+1}}{1 + (K_1 - 1)a_i - K_1(a_i)^{\nu+1}}\right) \qquad [27]$$

where $\lambda_{i,m}$ is an empirical solvation parameter to better account for the sorption between the two limiting cases. For a pure component sorption of saturated vapor or liquid, $a_i = 1$, the strongly bound molecules, thus, are

$$\lambda_i^{C,sat} = \lambda_{i,m}\frac{1 + \nu}{2\left(1 + \frac{1}{K_1\nu}\right)} \approx \lambda_{i,m}\frac{1 + \nu}{2} \qquad [28]$$

which provides an interrelation between $\lambda_{i,m}$ and υ.

An implicit expression is obtained for the sorption of liquid in terms of activity $a_{i,L}$ by first combining Eq. 27 with Eq. 1, and then substituting to Eq. 12 and 13 with 14, and finally substituting the activity and pressure expressions to Eq. 6

$$\left\{\lambda_{i,L} - \frac{\lambda_{i,m}K_1 a_{i,L}}{(1 - a_{i,L})}\left[\frac{1 - (\nu + 1)(a_{i,L})^\nu + \upsilon(a_{i,L})^{\nu+1}}{1 + (K_1 - 1)a_{i,L} - K_1(a_{i,L})^{\nu+1}}\right]\right\}^{-1}$$
$$= a_{i,L}^{-1}\exp\left\{\frac{\overline{V}_i}{RT}\left(\frac{\kappa\lambda_{i,L}}{\lambda_{i,L} + V_M/V_i}\right)\right\} - 1 \qquad [29]$$

while for the case of the vapor-phase sorption, the final expression is

$$\left\{\lambda_{i,V} - \frac{\lambda_{i,m}K_1 a_{i,V}}{(1 - a_{i,V})}\left[\frac{1 - (\nu + 1)(a_{i,V})^\nu + \nu(a_{i,V})^{\nu+1}}{1 + (K_1 - 1)a_{i,V} - K_1(a_{i,V})^{\nu+1}}\right]\right\}^{-1}$$
$$= a_{i,V}^{-1}\exp\left\{\frac{\overline{V}_i}{RT}\left[\frac{\kappa\lambda_{i,V}}{\lambda_{i,V} + V_M/V_i} - (S\sigma\cos\theta)\right.\right.$$
$$\left.\left.\times\left(1 + \frac{\overline{V}_M}{V_i}\frac{1}{\lambda_{i,V}}\right)\right]\right\} - 1 \qquad [30]$$

Thus, for a given $\lambda_{i,m}$, K_1, ν, $\overline{V}_i$, κ, S, σ, θ, and $\overline{V}_M$, the sorption isotherm can be determined for vapor or liquid phase sorption. Further, it is then clear from Eq. 29 and 30 that the solvent loading in liquid sorption, $\lambda_{i,L}$, would in general be different from the solvent loading from the vapor sorption $\lambda_{i,V}$.

Results and Discussion

In order to apply this model to water sorption in Nafion, the parameters K_1, $\lambda_{i,m}$, and ν, are determined based on the following considerations. The equilibrium constant K_1 between water and the side chain of SO_3H is approximated by that of sulfuric acid in water for the first ionization. Although different values of the ionization constants have been proposed,[45,51,52] the number of strongly bound solvent molecules, which can be determined separately by several techniques, is not substantially affected by the choice of the equilibrium constant, which is taken as 100. The solvent loading parameter, $\lambda_{i,m}$, is taken simply as the number of water molecules per acid site for monolayer coverage, because it provides for the correct value of chemically bound solvent molecules.[5,40] The number of equilibrium steps, ν, for hydration of the ions is related to the number of solvent molecules in the hydration shell by Eq. 27. The hydration number of a proton (H^+) is experimentally reported as 3.9 in sulfonated styrene-type ion exchanger,[49] or 4 by comparing the experimental variation of molar volume of water with theoretical variation based on the H_3O^+ ion association.[45] The number of water molecules in the hydration shell around sulfonic acid in Nafion membrane is also reported to be from 2 to 5, depending on the type of cations coexisting with the sulfonic acid. For example, two water molecules are found to be strongly bound per SO_3^- side chain for K^+-exchanged Nafion membrane, whereas for Na^+ and Li^+ membrane the number increases to 3-5 molecules.[53] Thus, the hydration number for Nafion is expected to be in a range of 4-6 in the fully hydrated state. For sulfonated styrene-type ion exchanger, a hydration number of 6 for the SO_3H group is reported experimentally,[54] and recent molecular modeling studies also result in a hydration number of 5-6 for SO_3H.[55,56] The activity of water in Nafion that is osmotically active is limited to the water molecules that are outside of the first hydration shell. Under dry or low-humidity conditions, only a few water

Table II. Parameter values employed in the model for the sorption of water in Nafion membrane.

Parameter	Value	Unit	Comment and references
$\overline{V}_M$	537	cm^3/mol	Partial molar volume of Nafion[5,14]
$\overline{V}_i$	18	cm^3/mol	Partial molar volume of water
S	210	m^2/cm^3	Specific pore surface area[57]
K_1	100	Dimensionless	The first ionization constant of sulfuric acid[5,45,50,51]
ν	4-6	Dimensionless	Number of chemical equilibrium steps of reaction[52-55]
$\lambda_{i,m}$	1.8	Dimensionless	Monolayer coverage being bound[5]
σ	72.1	mN/m	Surface tension of water[36,43]
θ	98	Dimensionless	Contact angle of saturated water vapor in Nafion[47]
κ	183	atm	Calculated assuming five hydration waters per acid group

molecules are in the hydration shell and are not enough to shield the ions. As the humidity increases, more water molecules become involved in the shielding of sulfonic acid and hydronium ion.

The mean pore radius of liquid-filled pores, r_p, is obtained in terms of λ_i by combining Eq. 14 and 15. The average pore radius of Nafion resulting from this model is 2 nm. The pore size increases with humidity and becomes 4 nm when the membrane is in equilibrium with liquid water. The variation of pore radius with solvent uptake is consistent with what is observed in Nafion by the standard porosimetry method (SPM,[57] ~2 nm), transmission electron microscopy (TEM,[58] ~2.5 nm), small angle scattering with neutrons (SANS) and X-rays (SAXS,[59,60] ~2.5 nm), and atomic force microscopy (AFM,[61] ~7.5 nm). Although larger pore/cluster aggregates are observed,[57,62] the mean pore radius of up to 4 nm used in this model is in good agreement with the reported data.

The surface of Nafion shows topographic features of nanophase-separated crystalline fluorocarbon, amorphous fluorocarbon, and ionic domains. When the surface is exposed to increasing humidity, the pore size as well as the surface roughness increases, as observed by SAXS/SANS[60] and AFM.[61] Therefore, the surface in a humid environment may be expected to exhibit a larger contact angle as compared with dry condition in light of Wenzel's law[63]

$$\cos\theta_{rough} = \gamma \cos\theta_{flat} \qquad [31]$$

where γ is the roughness factor, defined as the ratio of the actual area of a rough surface to the geometric projected area, and θ_{rough} and θ_{flat} are effective contact angles on rough and flat surfaces, respectively. Because γ is always larger than unity and the contact angle for vapor phase sorption is greater than 90°, it is expected that the contact angle would be increased by humidification.[43,64] However, the contact angle is actually found to decrease as the humidity increases because of the increased hydrophilicity of the surface.[47,65] The absorbed water in Nafion interacts with the side chain sulfonic acid groups as well as the fluorocarbon backbone and changes the nanostructure of Nafion to favor further adherence of water molecules, resulting in increased wettability or low contact angles. Although the inside wall of the pore is also not uniform, the contact angle in the pores is assumed to be similar to that of the surface.

The effective spring constant κ is obtained by assuming that five water molecules are strongly bound around an acid site in Nafion for liquid sorption. Thus, substitution of $x_{i,L} = 1.0$, $\lambda_i = 22$, and $\lambda_i^F = 17$ to Eq. 11-14 provides the effective spring constant κ of 183 atm. The effective spring constant κ varies with the elastic properties of the polymer matrix and interaction between the solvent molecules and the polymer structure.

The isotherm of water in Nafion as predicted by Eq. 30 as a function of humidity using the parameters listed in Table II is shown in Fig. 4 along with the experimental data from various groups.[11,14,16,18] In the initial sorption stage, about the first two water molecules per ion are sorbed at the activity (or relative humidity) of water $a_{i,V} = 0.1$. A high enthalpy change is known to occur for the sorption of the first and second water molecules. However, the hydration energy decreases very quickly as the number of water molecules in the primary shell increases.[66] After the strong sorption of water molecules in the initial stages, the solvent loading increases less steeply with activity and reaches $\lambda_{i,V} = 5\text{-}7$ at $a_{i,V} = 0.7\text{-}0.8$. In the high-activity region above $a_{i,V} = 0.8$, the sorption of water is very sensitive to the activity of the external water vapor and reaches $\lambda_{i,V}^{sat} = 14.9$ at saturation. In this high-activity region, the water molecules are largely physically sorbed. Generally, the large ions sorb less solvent molecules in the high-activity region because they occupy the space which otherwise would be taken up by the free solvent molecules. The model thus predicts the sorption of water in Nafion quite precisely throughout the entire range of vapor phase activity, including all the characteristic features, namely, the high initial slope, gradual increase of the slope after the sorption of the first few molecules, and high slope at activities above $a_{i,V} = 0.7\text{-}0.8$.

In order to explain Schroeder's paradox for the sorption of water in Nafion, Eq. 29 and 30 are reduced, respectively, for the sorption of pure liquid i, with $a_{i,L} = 1.0$ and Eq. 28 to

$$\left[\lambda_{i,L}^{sat} - \frac{\lambda_{i,m}(1+\nu)}{2}\right]^{-1} = \exp\left[\frac{\overline{V}_i}{RT}\left(\frac{\kappa\lambda_{i,L}^{sat}}{\frac{V_M}{V_i} + \lambda_{i,L}^{sat}}\right)\right] - 1 \qquad [32]$$

and for the sorption of saturated vapor of pure component, with $a_{i,V} = 1.0$ and Eq. 28 to

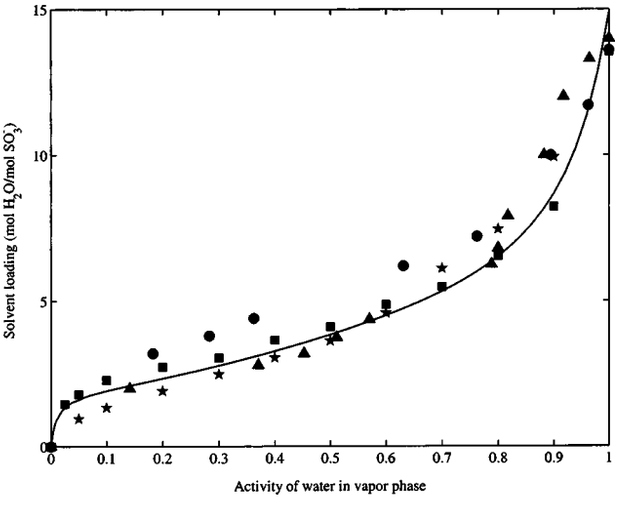

Figure 4. Prediction of the water sorption in Nafion (EW 1100) by the model (Eq. 30) taking ν=5 together with experimental observations: (——) model prediction, (▲) Ref. 12, (■) Ref. 14, (●) Ref. 16, and (★) Ref. 18.

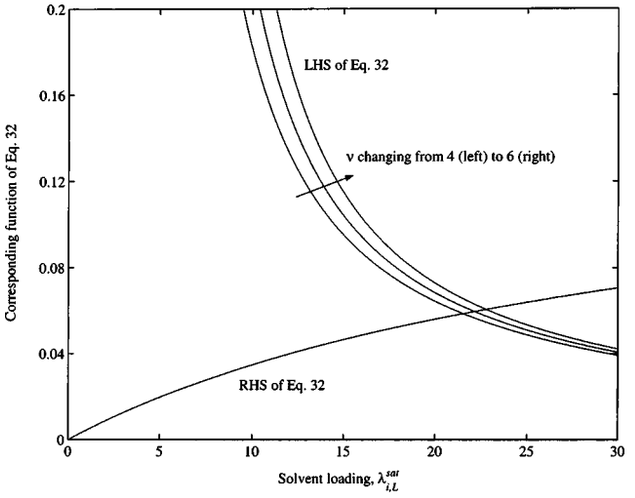

Figure 5. Prediction of water loading from liquid immersion with different equilibrium steps varying from 4 to 6 (Eq. 32).

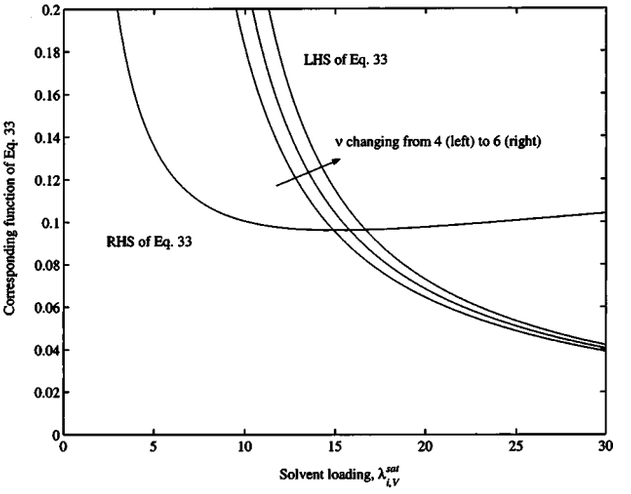

Figure 6. Prediction of water loading from vapor sorption with different equilibrium steps varying from 4 to 6 (Eq. 33).

$$\left[\lambda_{i,V}^{sat} - \frac{\lambda_{i,m}(1+\nu)}{2}\right]^{-1} = \exp\left\{\frac{\overline{V}_i}{RT}\left[\left(\frac{\kappa\lambda_{i,V}^{sat}}{\frac{V_M}{V_i} + \lambda_{i,V}^{sat}} - (S\sigma\cos\theta)\right) \times \left(1 + \frac{\overline{V}_M}{V_i}\frac{1}{\lambda_{i,V}^{sat}}\right)\right]\right\} - 1 \quad [33]$$

It can be inferred from Eq. 32 and 33 that the solvent loadings from the liquid, $\lambda_{i,L}^{sat}$, and that from saturated vapor, $\lambda_{i,V}^{sat}$, are different in general, which explains Schroeder's paradox. The reason for this difference is the surface energy of the vapor-liquid interface that affects the chemical potential of the sorbed phase for the case of saturated vapor sorption.

Figure 5 shows the solvent loading from the liquid sorption, $\lambda_{i,L}^{sat}$, with changing ν from 4 to 6. The left-hand side (LHS) and right-hand side (RHS) of Eq. 32 are plotted *vs.* $\lambda_{i,L}^{sat}$ and the solvent loading for the liquid sorption can be obtained by the intersection of the plots for different ν. The model predicts the loading of water $\lambda_{i,L}^{sat} = 22\text{-}23$ as ν changes from 4 to 6 as shown in Fig. 5. In the case of sorption of water vapor, each side of Eq. 33 is plotted *vs.* $\lambda_{i,V}^{sat}$ in Fig. 6. At saturated vapor condition, the model predicts the loading of water $\lambda_{i,V}^{sat} = 15\text{-}16$, as shown by the intersection of the plots of LHS and RHS for different values of ν in Eq. 33. There is a clear difference in solvent uptake between liquid and saturated vapor sorption; that is, the solvent uptake of vapor-phase sorption is less than that of liquid phase. In this case, the difference in λ is about seven, *i.e.*, seven fewer water molecules per acid site on average are sorbed in Nafion when the molecules are sorbed from the saturated vapor as compared with that from the liquid phase. When the membrane is removed from liquid water and exposed to saturated vapor, some of the water within the membrane evaporates, the vapor-liquid interface is created at the pore mouth, and the pore radius is reduced by 1 nm. A new equilibrium is established with fewer water molecules within Nafion. The size of clusters is decreased and the number of smaller clusters is increased, as inferred from AFM analysis under different humidity conditions.[61,62] Hence, the model provides a plausible explanation for Schroeder's paradox.

The model presented here predicts the entire isotherm, the solvent loadings from the vapor and liquid phase sorption, and explains Schroeder's paradox for water sorption in Nafion satisfactorily. In principle, the model can be applied to Nafion of different concentrations of acid sites, *e.g.*, equivalent weights (EWs) from 750 to 1500, different solvents, *e.g.*, methanol, cation-exchanged forms (K^+, Na^+, and Cs^+, etc.), as well as other polymers of different strength of acid sites, nature of chemical units, and elasticity, etc., provided the corresponding model parameters are available. Currently, the model is being further improved to separately account for the effects of polymer elasticity and the interaction between the solvent molecules and polymer, which have been combined in the effective spring constant κ, in terms of known polymer properties such as shear modulus and the solubility parameters for the interaction of solvent with each chemical unit of the polymer. It is also conceivable that the effect of pretreatment may be accounted for through the viscoelastic behavior of the membrane.

Conclusions

A physically plausible thermodynamic model is developed here for the sorption of solvent in a PEM. The sorption isotherm is a result of equilibrium established in the polymer-solvent system when the swelling pressure due to the uptake of solvent is balanced by the surface and elastic deformation pressures that restrain further stretching of the polymer network. The swelling pressure is obtained from the solvent activity within the polymer membrane and the dissociation characteristics of the ion-exchange site. This model predicts the isotherm of water in Nafion quite precisely and provides insights into the sorption phenomena in the ion-exchange polymers. The derived isotherm equations clearly show the difference in the sorbed amount from the liquid and its saturated vapor based on the surface energy of the vapor-liquid interface, thus providing a reasonable explanation for Schroeder's paradox.

Worcester Polytechnic Institute assisted in meeting the publication costs of this article.

References

1. P. Costamagna and S. Srinivasan, *J. Power Sources*, **102**, 242 (2001).
2. C. Stone and A. E. Morrison, *Solid State Ionics*, **152-153**, 1 (2002).
3. M. L. Perry and T. F. Fuller, *J. Electrochem. Soc.*, **149**, S59 (2002).
4. W. Grot, *Encyclopedia of Polymer Science and Engineering*, Vol. 6, 2nd ed., John Wiley & Sons, Inc., New York (1989).
5. T. Thampan, S. Malhotra, H. Tang, and R. Datta, *J. Electrochem. Soc.*, **147**, 3242 (2000).
6. G. Pourcelly, A. Oikonomen, C. Gavach, and H. D. Hurwitz, *J. Electroanal. Chem. Interfacial Electrochem.*, **287**, 43 (1990).
7. A. V. Anantaraman and C. L. Gardner, *J. Electroanal. Chem.*, **414**, 115 (1996).

8. W. Y. Hsu and T. D. Gierke, *Macromolecules*, **15**, 101 (1982).
9. R. S. Yeo and A. Eisenberg, *J. Appl. Polym. Sci.*, **21**, 875 (1977).
10. R. S. Yeo and H. L. Yeager, in *Modern Aspects of Electrochemistry*, Vol. 16, B. E. Conway, R. E. White, and J. O'M. Bockris, Editors, p. 451, Plenum Press, New York (1985).
11. T. A. Zawodzinski, C. Derouin, S. Radzinski, R. J. Sherman, V. T. Smith, T. E. Springer, and S. Gottesfeld, *J. Electrochem. Soc.*, **140**, 1041 (1993).
12. T. A. Zawodzinski, T. E. Springer, J. Davey, R. Jestel, C. Lopez, J. Valerio, and S. Gottesfeld, *J. Electrochem. Soc.*, **140**, 1981 (1993).
13. J. T. Hinatsu, M. Mizuhata, and H. Takenaka, *J. Electrochem. Soc.*, **141**, 1493 (1994).
14. D. R. Morris and X. Sun, *J. Appl. Polym. Sci.*, **50**, 1445 (1993).
15. E. Skou, P. Kauranen, and J. Hentschel, *Solid State Ionics*, **97**, 333 (1997).
16. K. K. Pushpa, D. Nandan, and R. M. Iyer, *J. Chem. Soc., Faraday Trans.*, **84**, 2047 (1988).
17. A. Steck and H. L. Yeager, *Anal. Chem.*, **52**, 1215 (1980).
18. D. Rivin, C. E. Kendrick, P. W. Gibson, and N. S. Schneider, *Polymer*, **42**, 623 (2001).
19. P. V. Schroeder, *Z. Phys. Chem.*, **45**, 75 (1903).
20. W. D. Bancroft, *J. Phys. Chem. Ithaca*, **16**, 395 (1912).
21. L. K. Wolff and E. H. Buchner, *Z. Phys. Chem.*, **89**, 271 (1915).
22. J. W. G. Musty, R. E. Pattle, and P. J. A. Smith, *J. Appl. Chem.*, **16**, 221 (1966).
23. H. Freundlich, *Colloid and Capillary Chemistry*, 3rd ed., p. 672, Methuen, London (1926).
24. R. C. Benning, R. J. Lee, J. F. Jennings, and E. C. Martin, *I&EC Process Des. Dev.*, **53**, 45 (1961).
25. P. Stamberger, *The Colloid Chemistry of Rubber*, p. 40, Oxford University Press, London (1929).
26. A. A. Tager, M. V. Tsilipotkina, L. V. Adamova, and L. K. Kolmakova, *Vysokomol. Soedin., Ser. B*, **16B**, 911 (1974).
27. J. Reilly and W. N. Rae, *Physico-Chemical Methods*, Vol. III, p. 364, D. Van Nostrand Company, Inc., New York (1948).
28. V. Freger, E. Korin, J. Winiak, and E. Korngold, *J. Membr. Sci.*, **164**, 251 (2000).
29. C. M. Gates and J. Newman, *AIChE J.*, **46**, 2076 (2000).
30. C. Tsonos, L. Apekis, and P. Pissis, *J. Mater. Sci.*, **35**, 5957 (2000).
31. P. Futerko and I.-M. Hsing, *J. Electrochem. Soc.*, **146**, 2049 (1999).
32. T. E. Springer, T. A. Zawodzinski, and S. Gottesfeld, *J. Electrochem. Soc.*, **138**, 2334 (1991).
33. H. P. Gregor, *J. Am. Chem. Soc.*, **70**, 1293 (1948).
34. H. P. Gregor, *J. Am. Chem. Soc.*, **73**, 642 (1951).
35. H. Helfferich, *Ion Exchange*, McGraw-Hill, New York (1962).
36. P. W. Atkins, *Physical Chemistry*, 3rd ed., W. H. Freeman and Company, New York (1986).
37. K. A. Mauritz and C. E. Rogers, *Macromolecules*, **18**, 483 (1985).
38. W. G. McMillan and J. E. Mayer, *J. Chem. Phys.*, **13**, 276 (1945).
39. P. J. Flory, *Principles of Polymer Chemistry*, Cornell University Press, Ithaca, NY (1953).
40. M. A. Yousef, R. Datta, and V. G. J. Rodgers, *AIChE J.*, **48**, 1301 (2002).
41. W. M. Kulicke and H. Nottlemann, *Polymers in Aqueous Media*, Advances in Chemistry Series 223, J. E. Glass, Editor, American Chemical Society, Washington, DC (1989).
42. D. A. Fridrikhsberg, *A Course in Colloid Chemistry*, Mir Publishers, Moscow (1986).
43. A. W. Adamson and A. P. Gast, *Physical Chemistry of Surfaces*, John Wiley & Sons, Inc., New York (1997).
44. J. C. Frazer and R. T. Myrick, *J. Am. Chem. Soc.*, **38**, 1907 (1916).
45. J. O'M. Bockris and A. K. N. Reddy, *Modern Electrochemistry*, Plenum Press, New York (1970).
46. G. E. Boyd and B. A. Soldano, *Z. Elektrochem.*, **57**, 162 (1953).
47. T. A. Zawodzinski, S. Gottesfeld, S. Shoichet, and T. J. McCarthy, *J. Appl. Electrochem.*, **23**, 86 (1993).
48. R. Buzzoni, S. Bordiga, G. Ricchiardi, G. Spoto, and A. Zecchina, *J. Phys. Chem.*, **99**, 11937 (1995).
49. E. Glueckauf and G. P. Kitt, *Proc. R. Soc. London, Ser. A*, **228**, 322 (1955).
50. R. M. Barrer, N. Mackenzie, and D. Macleod, *J. Chem. Soc.*, **2**, 1736 (1952).
51. M. Liler, *Reaction Mechanisms in Sulfuric Acid and Other Strong Acid Solutions*, Academic Press, New York (1971).
52. P. Atkins and L. Jones, *Chemical Principles: The Quest for Insight*, Freeman, New York (1998).
53. S. R. Lowry and K. A. Mauritz, *J. Am. Chem. Soc.*, **102**, 4665 (1980).
54. K. W. Pepper and D. Reichenberg, *Z. Elektrochem.*, **57**, 183 (1953).
55. A. Vishnyakov and A. V. Neimark, *J. Phys. Chem. B*, **104**, 4471 (2000).
56. S. J. Paddison, R. Paul, and T. A. Zawodinski, *J. Electrochem. Soc.*, **147**, 617 (2000).
57. J. Divisek, M. Eikerling, V. Mazin, H. Schmitz, U. Stimming, and Yu. M. Volfkovich, *J. Electrochem. Soc.*, **145**, 2677 (1998).
58. Z. Porat, J. R. Fryer, M. Huxham, and I. Rubinstein, *J. Phys. Chem.*, **99**, 4667 (1995).
59. T. D. Gierke, G. E. Munn, and F. C. Wilson, *J. Polym. Sci., Polym. Phys. Ed.*, **19**, 1687 (1981).
60. G. Gabel, *Polymer*, **41**, 5829 (2000).
61. R. S. Mclean, M. Doyle, and B. B. Sauer, *Macromolecules*, **33**, 6541 (2000).
62. P. J. James, T. J. McMaster, J. M. Newton, and M. J. Miles, *Polymer*, **41**, 4223 (2000).
63. R. N. Wenzel, *I&EC Process Des. Dev.*, **28**, 988 (1936).
64. S. R. Coulson, I. Woodward, J. P. S. Badyal, S. A. Brewer, and C. Willis, *J. Phys. Chem.*, **104**, 98836 (2000).
65. S. H. Anastasiadis, H. Retsos, S. Pispas, N. Hadjichristidis, and S. Neophytides, *Macromolecules*, **36**, 1994 (2003).
66. P. Kebarle, S. K. Searles, A. Zolla, J. Scarborough, and M. Arshadi, *J. Am. Chem. Soc.*, **89**, 6393 (1967).